Wave Dynamical Chaos in a Superconducting Three-Dimensional Sinai Billiard

H. Alt[1], C. Dembowski[1], H.-D. Gräf[1], R. Hofferbert[1],
H. Rehfeld[1], A. Richter[1], R. Schuhmann[2], and T. Weiland[2]
[1] *Institut für Kernphysik, Technische Hochschule Darmstadt,*
[2] *Fachgebiet Theorie Elektromagnetischer Felder, Technische Hochschule Darmstadt,*
D-64289 Darmstadt, Germany
(February 5, 2008)

Based on very accurate measurements performed on a superconducting microwave resonator shaped like a desymmetrized three-dimensional (3D) Sinai billiard, we investigate for the first time spectral properties of the vectorial Helmholtz, i.e. non-quantum wave equation for a classically totally chaotic and theoretically precisely studied system. We are thereby able to generalize some aspects of quantum chaos and present some results which are consequences of the polarization features of the electromagnetic waves.

PACS number(s): 05.45.+b, 41.20.Bt, 41.20.Jb

For nearly 20 years, billiard systems have provided a very effective tool for the investigation of semiclassical quantization of conservative chaotic systems [1,2]. This is due to the fact that even two-dimensional (2D) billiards (as opposed to billiards of higher dimensionality) are able to model a wide range of fully ergodic systems in Gutzwiller's sense of "hard chaos" [3]. As a matter of fact, properties of the wave dynamical spectra of such low-dimensional but classically non-integrable systems are fully described by the Gaussian Orthogonal Ensemble (GOE) of Random Matrix Theory (RMT) [4,5] if the underlying motion is invariant under time-reversal. On the other hand, classically regular, i.e. integrable systems lead to totally uncorrelated spectra.

Up to now investigations on chaotic 3D-billiards were performed in experiments with electromagnetic [6,7] and acoustic [8,9] waves, whereas the hardly feasible numerical modelling was restricted to very special geometries of high symmetry for the pure Schrödinger problem [10].

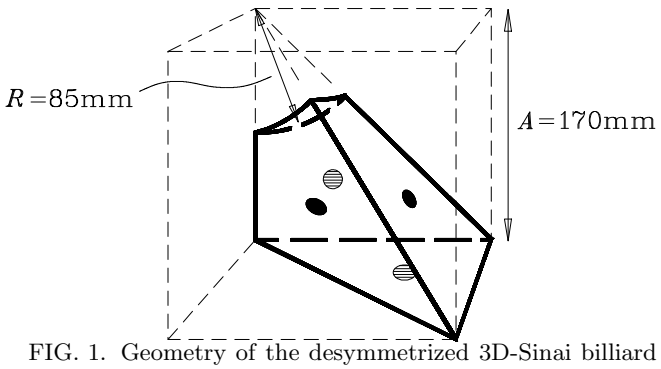

FIG. 1. Geometry of the desymmetrized 3D-Sinai billiard (boldface line) which constitutes one sixth of the dashed cube. Eight of those cubes form the full system. As indicated in the figure, one antenna was located in the center of each plane surface of the cavity.

The goal of the present paper is to provide for the first time a detailed analysis of a fully chaotic three-dimensional (3D) electromagnetic billiard with a classically well-known and theoretically precisely studied geometry: the 3D-Sinai billiard resp its desymmetrized version given by 1/48 of a cube with a sphere in its center, see Fig.1. The system has to be described by the time-independent, fully vectorial Helmholtz equation with electromagnetic boundary conditions. The same geometry was recently investigated numerically in the quantum regime [10] described by the time-independent Schrödinger equation and experimentally with acoustic waves [9]. Our analysis therefore allows a very distinct comparison of totally different wave dynamical phenomena in a system with exactly the same classical analogue. Our results should agree with those of [10] and [9] if the conjecture holds that RMT is adequate to describe spectra of arbitrary wave phenomena.

As several 2D- and 3D-billiards before [7,11–13], the electromagnetic resonator was made of Niobium which becomes superconducting below 9.2 K. This feature tremendously increases the resolution of the measured spectra due to quality factors of up to 10^7 compared to 10^3 in normal conducting resonators and signal-to-noise ratios of up to 70 dB. The resonator was cooled down to a temperature of 4.2 K and finally evacuated to a pressure of 0.2 mbar inside a bath cryostat. We were able to excite the cavity via four different antennas up to a frequency limit of 20 GHz given by our HP8510B vector network analyzer which was used for the generation and detection of the microwave signal. Either the reflected signal from one antenna, or the transmitted signal between two different antennas was measured. Figure 2 shows a typical transmission spectrum between 6.50 and 6.75 GHz. Identifying accurately per hand the positions of significant peaks of every single spectrum and performing in the next step a detailed comparison of all the possible spectra, a total set of 1881 experimental eigenmodes was obtained which form the base of the following investigations.

To check for the mechanical accuracy of the cavity and to estimate the effects due to the coupling of the isolated resonator to the external world (coupling holes and slightly penetrating coupling wires of the rf-cables), we also simulated the spectrum using the electromagnetic CAD-program MAFIA (solution of Maxwell's equation by the Finite Integration Algorithm [14]). The resonator was modelled using a mesh consisting of 10^6 points, and a full 3D broadband time domain calculation with a total number of 150,000 time steps was performed. A task which is feasible on a standard workstation with one week of CPU time. The eigenfrequencies were finally determined by a Fast Fourier Transform yielding a resolution of about 1.2 MHz over a wide frequency range. Limited by this resolution a comparison with the experimental spectrum (with a resolution of 10 kHz) allows a one-to-one correspondence between simulation and experiment within a region up to 7.5 GHz including 94 resonances.

For comparison, the numerically simulated eigenfrequencies are given as dashed vertical lines in Fig.2. As a matter of fact the experimental eigenfrequencies are systematically up-shifted due to the contraction of the resonator during the cool-down. From this shift (linearly increasing with frequency) we extracted the relative contraction coefficient $(\Delta x/x)_{exp} \approx 2.0 \cdot 10^{-3}$ which is close to the value for Niobium as given in the literature [15], $(\Delta x/x)_{lit} \approx 1.4 \cdot 10^{-3}$. Beside this effect, every experimental resonance is individually shifted due to the coupling holes and antennas and the mechanical fabrication tolerances. However, these individual shifts are on the order of some $5 \cdot 10^{-4}$ and thus much smaller than the effect of the cool-down.

To prepare the experimental spectrum of extracted eigenfrequencies for the statistical analysis, we first unfolded it, i.e. rescaled the frequency axis to a mean level spacing of unity. According to this, in applying the generalized electromagnetic Weyl formula [16,17]

$$N^{smooth}(f) \approx \frac{8\pi}{3c_0^3} V \cdot f^3 - \left(\frac{4}{3\pi c_0} \int \frac{d\sigma}{R} - \frac{1}{6\pi c_0} \int da \frac{(\pi - \Omega)(\pi - 5\Omega)}{\Omega} \right) \cdot f + const. \quad (1)$$

to describe the smooth part of the integrated level density (spectral staircase), the spectrum is again checked for completeness. Here, N counts the total number of resonances up to a certain frequency f, V denotes the volume of the geometry and c_0 is the speed of light. In the linear term, R labels the mean radius of curvature over the surface σ and Ω is the dihedral angle along the edges a. Note that the leading cubic term of this expression is twice the corresponding term in the scalar, i.e. quantum problem, and that there is no quadratic term . Both features are due to the vectorial character of the electromagnetic field inside the cavity and thus a consequence of two transverse polarizations of the electromagnetic wave. A comparision between Eq.(1) and the integrated experimental level density yields an estimate for the number of uncertain resonances $\Delta N \approx (V_{exp}/V_{theo} - 1)N_{total} \approx 4$. Here, N_{total} denotes the complete set of 1881 resonances. After the extraction of this smooth part the expected non-systematic fluctuations around zero could be observed, they are the carrier of all accessible information about the classical dynamics inside the billiard.

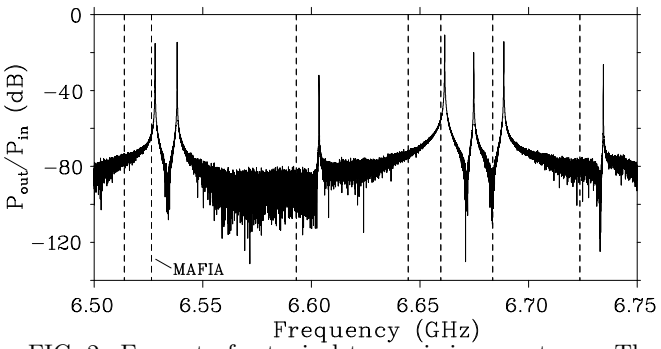

FIG. 2. Excerpt of a typical transmission spectrum. The signal displays the ratio of output power to input power on a logarithmic scale. The numerically simulated eigenfrequencies are given by dashed lines. The shift between experiment and simulation is mainly due to the contraction of the resonator during the cool-down.

Statistical measures developed to display the correlations embedded in these fluctuations were originally introduced in the 1950th to describe spectra of nuclear systems with many degrees of freedom. [4]. An adequate and widely tested statistical measure to examine short-range correlations up to a length of *one* mean level spacing is given by the nearest neighbour spacing distribution (NND), displaying the probability $P(s)$ for a certain spacing s of two adjacent resonances in the spectrum. Figure 3 (l.h.s.) displays $P(s)$ of the experimental spectrum as well as the two limiting curves, "Poisson" for a totally uncorrelated spectrum corresponding to regular motion on the classical side, and "GOE" for the totally chaotic case. Obviously, the experimental histogram is very close to the GOE distribution. In the next step we analyzed the spectrum on a larger scale in order to investigate long-range correlations. For this purpose we calculated $\Sigma^2(L)$, which expresses the variance of a number of resonances inside an interval of length L on the unfolded scale, as well as the related Dyson-Mehta statistics, $\Delta_3(L)$, also sensitive up to L, i.e. *several* mean level spacings. The result for both properties is given as well in Fig.3 (l.h.s.). Here, two observations can be made: First, the experimental curves rapidly deviate from the GOE prediction and lie in between the regular and the chaotic case, and second, above a certain value L_{max}, which is different for both statistics ($L_{max}^{\Sigma^2} \approx 40$, $L_{max}^{\Delta_3} \approx 150$), the experimental curves run into saturation. This last

feature is exactly what is expected from theory [18], displaying the fact that for increasing L the given statistics are more and more sensitive to specific, i.e. non-universal features of the system. In this sense L_{max} separates the universal scale which is dominated by the general dynamical behaviour of the classical analogue – described by the collective behaviour of all *long* periodic orbits of the system – from the non-universal scale which is generated by individual system-specific attributes – in the present case given by the *shortest* periodic orbits of the billiard. Note that the difference between L_{max} of Σ^2 and the value obtained for Δ_3 is $L_{max}^{\Delta_3} \approx 4 \cdot L_{max}^{\Sigma^2}$ [19], which is well reproduced by the given spectrum. Theoretically the length of the shortest periodic orbits l_{min} depends on $L_{max}^{\Delta_3}$ according to [7]

$$L_{max}^{\Delta_3} = \frac{3c_0}{l_{min} f_{max}} \frac{N_{total}}{2} \ , \qquad (2)$$

where f_{max} denotes the upper frequency limit of 20 GHz. Using the length of the first observable periodic orbit, l_{min}=0.34 m (see below), one estimates $L_{max}^{\Delta_3} \approx 125$, which is close to the value of Fig.3.

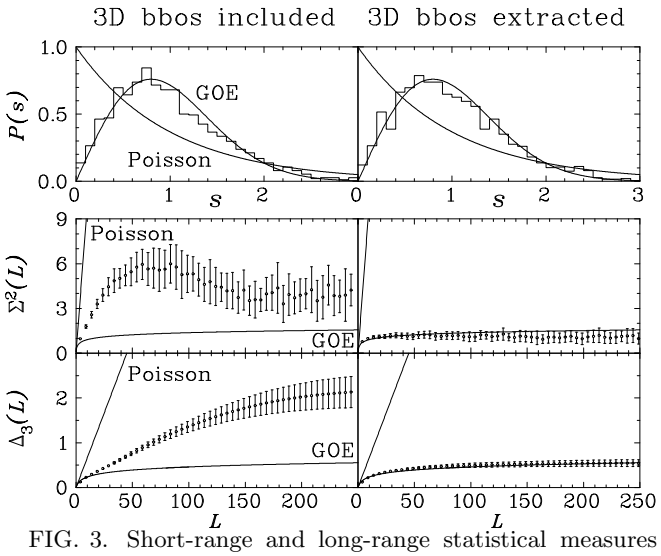

FIG. 3. Short-range and long-range statistical measures before and after the extraction of 3D bbos, see text.

To characterize all statistical measures more quantitatively and in order to check *how well* the GOE prediction describes the results, we also analyzed the experimental curves according to a model of Berry and Robnik [20] within the universal region. The basic intention of this model is to provide a continuous interpolation between the pure Poissonian and GOE using a mixing-parameter q which corresponds to the relative phase space volume that is covered by chaotic trajectories. In the present case we obtained for the three statistical measures on the l.h.s. of Fig.3 $q_{NND} = 0.95 \pm 0.01$, $q_{\Sigma^2} = 0.89 \pm 0.02$ and $q_{\Delta_3} = 0.91 \pm 0.02$, indicating a small but systematic deviation from unity, the limit for pure chaotic systems. Thus, although the system is fully ergodic on the classical side without any stable islands in phase space, the wave dynamical side pretends their existence. To understand this phenomenon, we analyzed the classical analogue in more detail. Therefore, we continued our investigation on a more specific scale which provides a bridge between the classical chaotic features and their impact on the electromagnetic spectrum. This scale is given by the length spectrum of the billiard, which is practically obtained through the Fourier transform of the spectral level density or its fluctuating part, respectively,

$$\tilde{\rho}^{fluc}(l) = \int_{f_{min}}^{f_{max}} \rho^{fluc}(f) \cdot \exp(i \frac{2\pi}{c_0} l f)\, df \ . \qquad (3)$$

Here l denotes the physical length scale. Since the property $\tilde{\rho}^{fluc}(l)$ maps the long periods in frequency space onto short scales in length space, the resulting spectrum shows peaks near the classical periodic orbits of the billiard. Figure 4 exhibits the lower part of this length spectrum up to l=1.5 m. Here a rich structure of peaks can be observed above a minimum length l_{min}=0.34 m. This first peak belongs to the shortest 3D bouncing ball orbit (3D bbo) of the billiard, propagating along one edge of the desymmetrized cube without striking the sphere, see sketch in the inset.

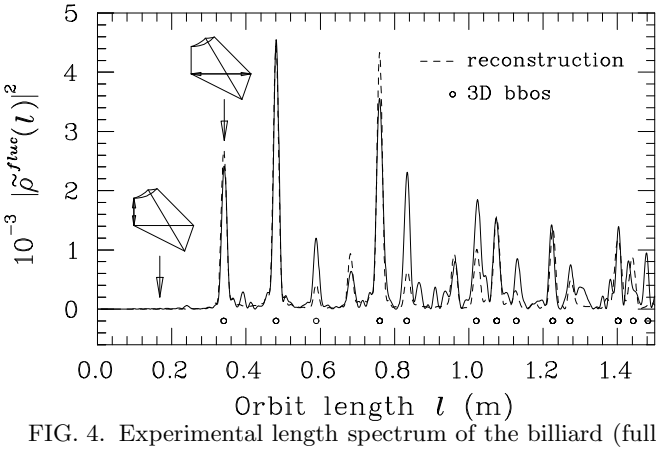

FIG. 4. Experimental length spectrum of the billiard (full line) and the semiclassical reconstruction using only 3D bbos (dashed line). The pictures in the inset show the first unstable and the first 3D bouncing ball orbit, respectively.

Exactly this shortest length was used to estimate the saturation parameter L_{max} of Δ_3 (see above). In fact, this first 3D bbo is the shortest non-isolated, neutrally stable periodic orbit of the system. It is highly remarkable, that this is not the first periodic orbit of the billiard. The shortest unstable periodic orbit runs along the shortest edge of the desymmetrized billiard which is intersected by the sphere, it possesses a length l_{min}^{upo}=0.17 m, see sketch in the inset. The corresponding peak in the Fourier spectrum is drastically suppressed due to the desymmetrization of the system itself [10,21]. As a matter of fact, the obtained length spectrum is totally dominated by bbos of all possible dimensions, not only in the

quantum case [10] but also in the electromagnetic counterpart. To demonstrate this, we considered the contribution of the leading 3D bbos to the given length spectrum. Therefore, we used a lattice vector description of Berry [22] to label and generate all 3D bbos up to a certain length and determined their contribution on $\rho_{bbo}^{fluc}(f) = dN_{bbo}^{fluc}/df$ through [7]

$$N_{bbo}^{\mathrm{fluc}}(X) = \frac{2\pi S_{bbo}}{l_{bbo}^2}\left(\sum_{0<n<X} \left(X^2 - n^2\right) - \frac{2}{3}X^3 + \frac{1}{2}X^2 \right) , \tag{4}$$

with $X = l_{bbo} f/c_0$. Here, the length of a given 3D bbo, l_{bbo}, was deduced directly from the lattice vector and S_{bbo}, the perpendicular area on which this orbit exists, was fixed in a Monte-Carlo simulation. In the given range up to l=1.5 m we obtained 55 3D bbos of different degeneracies and with positive S_{bbo}, their superimposed semiclassical reconstruction due to Eq.(4) is given by the dashed line in Fig.4. It is highly remarkable that nearly the full structure of the given length spectrum can be reproduced using only 3D bbos, whereas the influence of the enormous number of unstable periodic orbits (approximately 36000 up to l=1.5 m [23]) is hidden in the background. Discrepancies between the experimental length spectrum and the reconstruction can be predominantly found at the locations of the 3D bbos themselves and arise because of the existence of sub-dimensional and tangential bbo manifolds [10].

Finally, to demonstrate the influence of the considered 3D bbos on the statistical measures NND, Σ^2 and Δ_3, we repeated our statistical analysis using a modified unfolding procedure in which the standard Weylian, Eq.(1), is extracted together with the contribution of the 3D bbos, Eq.(4). For this we used all 3D bbos up to a length l=3.0 m. The result is given in Fig.3 (r.h.s.) displaying, now also for Σ^2 and Δ_3, nearly perfect agreement with the GOE prediction in the universal regime up to L_{max}. The corresponding, i.e. corrected mixing parameters, were fixed to be $q_{NND} = 0.96 \pm 0.01$, $q_{\Sigma^2} = 0.99 \pm 0.01$ and $q_{\Delta_3} = 0.99 \pm 0.01$.

In summary, a set of 1881 highly resolved eigenmodes of an electromagnetic 3D-Sinai billiard was analyzed according to standard methods of Random Matrix and Periodic Orbit Theory. Spectral correlations are shown to be totally consistent with the predictions of the GOE after the systematic extraction of the family of 3D bbos which dominate not only the length spectrum of the billiard but also lead to dramatic deviations from Gaussian characteristics in the measures for long-range correlations, Σ^2 and Δ_3.

We would like to thank H. Lengeler and the CERN workshops for the excellent fabrication of the cavity. We are very grateful to B. Eckhardt and H. Primack for a lot of suggestions, discussions and their theoretical cooperation. One of us (A.R.) thanks in particular U. Smilansky for providing him first with a one-to-one paper model of the desymmetrized 3D Sinai billiard of Fig.1 which led to the present investigations. We finally thank M. Köppen for providing us with the thermal contraction coefficient of niobium. This work has been supported by the Sonderforschungsbereich 185 "Nichtlineare Dynamik" of the Deutsche Forschungsgemeinschaft and in part by the Bundesministerium für Bildung und Forschung under contract number 06DA665I.

[1] S.W. McDonald and A.N. Kaufman, Phys. Rev. Lett. **42**, 1189 (1979).
[2] M.V. Berry, Proc. R. Soc. Lond. A**413**, 183 (1987).
[3] M.C. Gutzwiller, *Chaos in Classical and Quantum Mechanics* (Springer, New York, 1990).
[4] M.L. Mehta, *Random Matrices*, 2nd ed., (Academic Press, San Diego, 1991).
[5] O. Bohigas, in *Chaos and Quantum Physics*, M.-J. Giannoni, A. Voros, and J. Zinn-Justin, eds. (Elsevier, Amsterdam, 1991), p. 89.
[6] S. Deus, P.M. Koch and L. Sirko, Phys. Rev. E**52**, 1146 (1995).
[7] H. Alt, H.-D. Gräf, R. Hofferbert, C. Rangacharyulu, H. Rehfeld, A. Richter, P. Schardt, and A. Wirzba, Phys. Rev. E**54**, 2303 (1996).
[8] R.L. Weaver, J. Acoust. Soc. Am. **85**, 1005 (1989).
[9] C. Ellegaard, T. Guhr, K. Lindemann, H.Q. Lorensen, J. Nygård, and M. Oxborrow, Phys. Rev. Lett. **75**, 1546 (1995).
[10] H. Primack and U. Smilansky, Phys. Rev Lett. **74**, 4831 (1995).
[11] H.-D. Gräf, H.L. Harney, H. Lengeler, C.H. Lewenkopf, C. Rangacharyulu, A. Richter, P. Schardt, and H.A. Weidenmüller, Phys. Rev. Lett. **69**, 1296 (1992).
[12] H. Alt, H.-D. Gräf, H.L. Harney, R. Hofferbert, H. Lengeler, C. Rangacharyulu, A. Richter, and P. Schardt, Phys. Rev. E**50**, 1 (1994).
[13] H. Alt, H.-D. Gräf, H.L. Harney, R. Hofferbert, H. Lengeler, A. Richter, P. Schardt, and H.A. Weidenmüller, Phys. Rev. Lett. **74**, 62 (1995).
[14] T. Weiland, *International Journal of Numerical Modelling*, **9**, 295 (1996).
[15] H.D. Erfling, Ann. Physik **41**, 467 (1942).
[16] W. Lukosz, Z. *Physik* **262**, 327 (1973).
[17] R. Balian and B. Duplantier, Ann. of Phys. **104**, 300 (1977).
[18] M.V. Berry, Proc. R. Soc. Lond. A**400**, 229 (1985).
[19] A. Delon, R. Jost and M. Lombardi, J. Chem. Phys. **95**, 5701 (1991).
[20] M.V. Berry and M. Robnik, J. Phys. A**17**, 2413 (1984).
[21] O. Frank and B. Eckhardt, Phys. Rev. E**53**, 4166 (1996).
[22] M.V. Berry, Ann. Phys. **131**, 163 (1981).
[23] H. Primack, private communication (1996).